Nanotechnology Science and Technology

Ion-Synthesis of Silver Nanoparticles and their Optical Properties

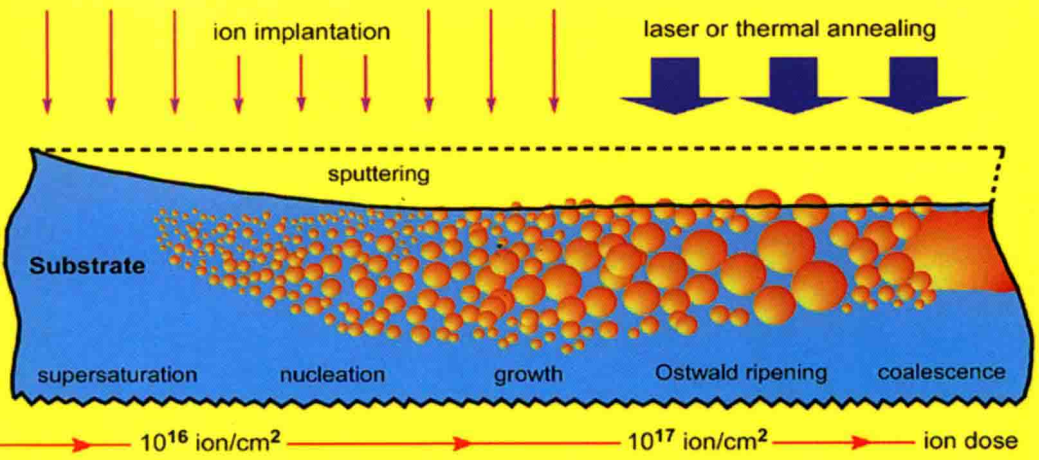

Andrey L. Stepanov

Novinka

NANOTECHNOLOGY SCIENCE AND TECHNOLOGY

ION-SYNTHESIS OF SILVER NANOPARTICLES AND THEIR OPTICAL PROPERTIES

ANDREY L. STEPANOV*
Kazan Physical-Technical Institute,
Russian Academy of Sciences,
Kazan, Russian Federation
Kazan State University, Kazan, Russian Federation

Nova Science Publishers, Inc.
New York

* e-mail: aanstep@gmail.com anstep@kfti.knc.ru

LIBRARY OF CONGRESS CATALOGING-IN-PUBLICATION DATA

Stepanov, Andrey L.
Ion-synthesis of silver nanoparticles and their optical properties /
Andrey L. Stepanov.
p. cm.
Includes index.
ISBN 978-1-61668-862-2 (softcover)
1. Silver--Optical properties. 2. Nanoparticles--Optical properties. 3. Dielectrics--Optical properties. 4. Ion implantation. 5. Ionic structure.
I. Title.
TA480.S5S74 2009
620.1'8923--dc22

2010016672

Published by Nova Science Publishers, Inc. † New York

NANOTECHNOLOGY SCIENCE AND TECHNOLOGY

ION-SYNTHESIS OF SILVER NANOPARTICLES AND THEIR OPTICAL PROPERTIES

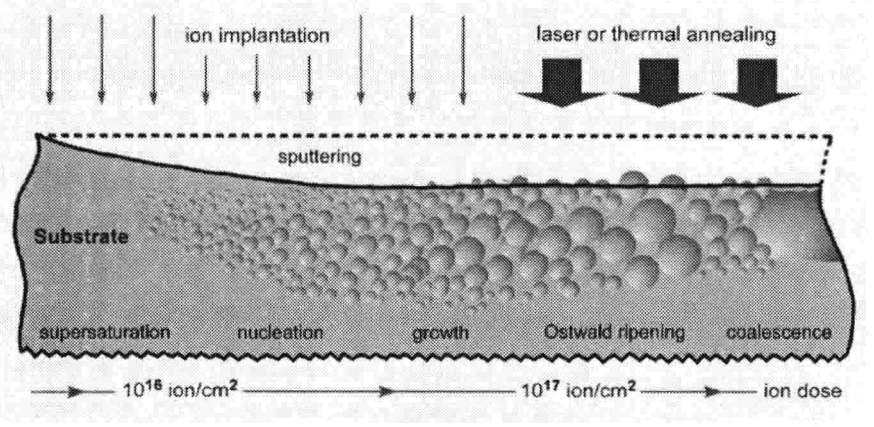

NANOTECHNOLOGY SCIENCE AND TECHNOLOGY

Additional books in this series can be found on Nova's website under the Series tab.

Additional E-books in this series can be found on Nova's website under the E-book tab.

ABSTRACT

Recent results on ion-synthesis by low-energy implantation and optical properties of silver nanoparticles in various dielectrics (glasses and polymers) and on the interaction of high-power laser pulses with such composite materials are reviewed. One of the features of composites prepared by the low-energy ion implantation is the growth of metal particles with a wide-size distribution in the thin depth from the irradiated substrate surface. This leads to specific optical properties of implanted materials, partially to difference in reflection measured form implanted and rear face of samples. The excimer laser pulse modification of silver nanoparticles fabricated in silicate glasses is considered. Pulsed laser irradiation makes it possible to modify such composite layer, improving the uniformity in the size distribution of the nanoparticles.The optical absorption of silver nanoparticles fabricated in polymer is also analysed. Unusual weak and broad plasmon resonance spectra of the nanoparticles are studied in the frame of the carbonisation of ion-irradiated polymer. Based on the Mie theory, optical extinction spectra for metal particles in the polymer and carbon matrices are simulated and compared with particle spectra for complex silver core–carbon shell nanoparticles. A new experimental data on nonlinear optical properties of synthesised silver nanoparticles are also presented.

INTRODUCTION

Nanomaterials are cornerstones of nanoscience and nanotechnology. The relevant feature size of nanomaterial components is on the order of a few to a few hundreds of nm. At the fundamental level, there is a real need to better understand the properties of materials on the nanoscale level. At the technological front, there is a strong demand to develop new techniques to fabricate and measure the properties of nanomaterials and relevant devices. Significant advancement was made over the last decades in both fronts. It was demonstrated that materials at the nanoscale have unique physical and chemical properties compared to their bulk counterparts and these properties are highly promising for a variety of technological applications. One of the most fascinating and useful aspects of nanomaterials is their optical properties. Applications based on optical properties of nanomaterials include optical detectors, laser, sensor, imaging, display, solar cell, photocatalysis, photoelectrochemistry, and biomedicine [1]. Among variety of nanomaterial a most fascinating ones are composite materials containing metallic nanoparticles (MNPs) which now considered as a basis for designing new photonic media for optoelectronics and nonlinear optics [2]. Simultaneously, with the search for and development of modern technologies intended for nanoparticle synthesis, substantial practical attention was devoted to designing techniques for controlling the MNP size. This is caused by the fact that the properties of MNPs, such as the quantum size effect, single-electron conduction, etc., which are required for various applications, take place up to a certain MNP size. An example of their application in optoelectronics is a prototype of integrated electronic circuit - chip that combines metallic wires as conductors of electric signals with fibers as guides of optical signals. In practice, light guides are frequently made of synthetic sapphire or siliconoxide,

which are deposited on or buried in semiconductor substrates. In this case, electrooptic emitters and that accomplish electric-to-optic signal conversion are fabricated inside the dielectric layer. This light signal from a microlaser is focused in a light guide and then transmitted through the optoelectronic chip to a high-speed photodetector, which converts the photon flux to the flux of electrons. It is expected that light guides used instead of metallic conductors will improve the data rate by at least two orders of magnitude. Moreover, there is good reason to believe that optical guide elements will reduce the energy consumption and heat dissipation, since metallic or semiconductor components of the circuits may be replaced by dielectric ones in this case. Prototype optoelectronic chips currently available are capable of handling data streams with a rate of 1 Gbit/s, with improvement until 10 Gbit/s in future. Key elements of dielectric waveguides used for light propagation are nonlinear optical switches, which must provide conversion of laser signal for pulse duration as short as pico- or femtoseconds. The nonlinear optical properties of MNP-containing dielectrics stem from the dependence of their refractive index and nonlinear absorption on incident light intensity [2, 3]. This effect is associated with MNPs, which exhibit an enhancement of local electromagnetic field in a composite and, as consequence, a high value of the third order nonlinear susceptibility when exposed to ultra-short laser pulses. Therefore, such MNP-containing dielectric materials may be used to advantage in integrated optoelectronic devices [4]. A local field enhancement in MNPs stimulates a strong linear optical absorption called as surface plasmon resonance (SPR). The electron transitions responsible for plasmon absorption in MNPs also cause a generation of an optical nonlinearity of a composite in the same spectral range. As a result, the manifestation of nonlinear optical properties is most efficient for wavelengths near the position of a SPR maximum. In practice, to reach the strong linear absorption of a composite in the SPR spectral region, attempts are made to increase the concentration (filling factor) of MNPs. Systems with a higher filling factor offer a higher nonlinear susceptibility, when all other parameters of composites being the same. Usually noble metals and copper are used to fabricate nonlinear optical materials with high values of third order susceptibility.

Small size alters the electronic structure of MNPs. This provides greater pumping efficiency and lower overall threshold for applications in optical switching. The potential advantages of MNP composites as photonic materials are substantial improvement in the signal switching speed up to 100 GHz repetition frequencies are expected in communication and computing systems of the 21st century[3]. Fig. 1 compares in graphical formthe switching speeds

and switching energies of a number of electronic and optical materials and devices (adapted from [3]). Within the broad range on parameters covered by "conventional semiconductor microelectronics", current metal-oxide-semiconductor field-effect transistor devices made in Si have low switching energies, but switching time in the nanosecond range. Photonic devices based on multiple quantum well (MQW) structures – SEED and GaAs MQW devices and Fabry-Perot (FP) cavities based on ferroelectric such as lithium niobate – have extremely low switching energies in comparison to MNPs, but relatively slow switching speed. As seen, MNPs fit into the area of current semiconductor electronics: they have very rapid switching times, as low as picoseconds and femtoseconds. Unfortunately, so far, still relatively little attention has been paid to the practical problems associated with the realization of electo-optical device structures on silicon platform— the analog of building up transistor structures (sources, gates, electrodes) for microelectronic applications.

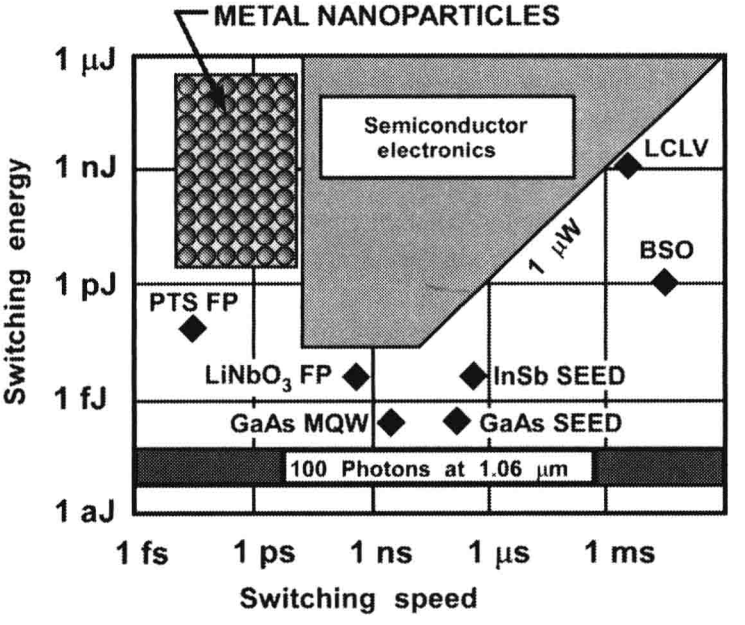

Figure 1. Plot of various photonic materials showing their switching energies and switching speeds.

There are variety ways to synthesis MNPs in dielectrics, such as magnetron sputtering, the convective method, ion exchange, sol–gel

deposition, etc. One of the most promising enhanced fabrication methods is ion implantation [5-9] because it allows reaching a high metal filling factor in an irradiated matrix beyond the equilibrium limit of metal solubility and provides controllable synthesis of MNPs at various depths under the substrate surface. Nearly any metal–dielectric composition may be produced using ion implantation. This method allows for strict control of the doping ion beam position on the sample surface with implant dose as, for example, in the case of electron- and ion-beam lithography. Today, ion implantation is widely used in industrial semiconductor chip fabrication. Therefore, the combination of MNP-containing dielectrics with semiconductor substrates by same technological approach as ion implantation could be reached quite effective. Moreover, ion implantation can be applied for different steps in optoelectronic material fabrication such as creation of optical waveguides by implantation with rear gas ions (H^+, He^+ etc.) [9], a designing of electric-to-optic signal convectors and microlaser by irradiation of dialectics waveguides with rear metal ions (Er^+, Eu^+ etc.) [9, 10] and a synthesis of MNPs (Fig. 2).

The history of MNP synthesis in dielectrics by ion implantation dates back to 1973, when a team of researchers at the Lyons University in France [11, 12] pioneered this method to create particles of various metals (sodium, calcium, etc.) in LiF and MgO ionic crystals. Later, ion-synthesis of noble nanoparticles was firstly done in study of Au- and Ag-irradiated lithia-alumina-silica glasses [13, 14]. Development was expanded from the metal implants to the use of many ions and the active formation of compounds, including metal alloys and totally different composition precipitate inclusions. In ion implantation practice, MNPs were fabricated in various materials, such as polymers, glass, artificial crystals, and minerals [15, 16]. By implantation, one can produce almost any metal–dielectric composite materials, as follows from Table 1, which gives a comprehensive list of references of various dielectrics with implanted silver nanoparticles with conditions for their fabrications.

The book focuses on recent advantages in fabrication of silver nanoparticles by low-energy in implantation in various inorganic matrixes [17-161]. Also, some examples of nonlinear optical repose in such composites are presented and discussed.

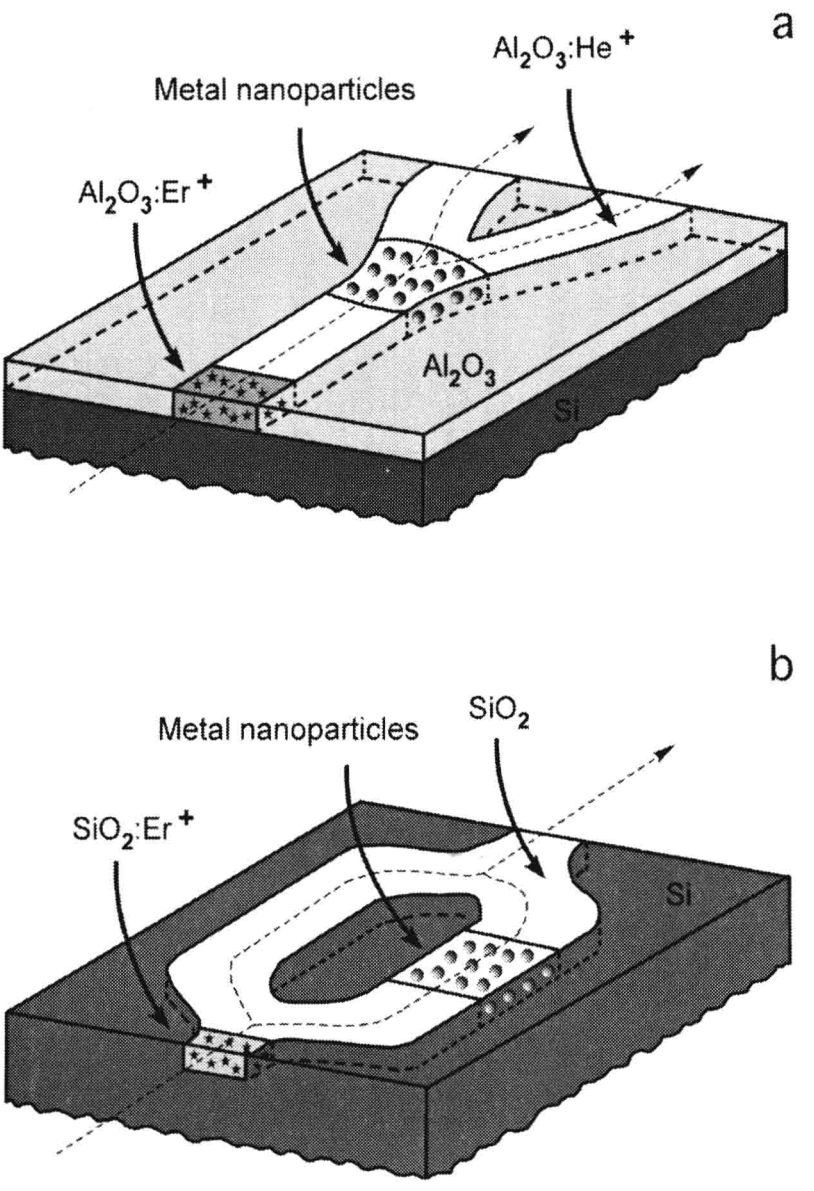

Figure 2.A prototype of optoelectronic chip with a dielectric waveguide combined with silicone substrate. Ion implantation can be applied to fabricate selective area doped by rear metal ions (marked by stars) to work as microlaser and to illuminate in waveguide, created by rear-gas ion radiation with MNPs to form an optical switcher.

Table 1. Types of dielectric inorganic matrix with silver nanoparticles synthesized by ion implantation combined in some cases with post-implantation heat treatment. Abbreviations – $2Ag_2O{\cdot}3Na_2O{\cdot}25ZnO{\cdot}70TeO_2$(ANZT glass), alkali-borosilicate glass (ABSG), borosilicate Pyrex glass (BPYR), soda-lime silicate glass (SLSG),yttria stabilized cubic zirconia (YSZ);optical reflection (OR), optical absorption (OA), transmission electron microscopy (TEM), TEM cross-section (TEM-CS), high resolution TEM (HRTEM), scanning transmission electron microscopy (STEM), conductivity measurements (CM), atom force microscopy (AFM), optical microscopy (OM), selected area electron diffraction (SAED), energy dispersiveX-ray spectrometry(EDS), high-resolution X-ray diffraction (XRD), Z-scan, RZ-scan by reflection, degenerate four wave mixing (DFWM); room temperature (RT).

Matrix type	Ion energy, keV	Ion dose,ion/cm^2	Current density,μA/см^2	Matrix temperature,°C	Post-implantation heat treatment	Methodsof particle detection	Authors
Al_2O_3 crystal <1010>	50 360	$4.0{\cdot}10^{16}$ $5.0{\cdot}10^{16}$ $8.0{\cdot}10^{16}$	1-5	77 K 300	Annealing in air at 650°C, 30 min.	OA	Rahmani *et al.* 1988 [17] 1989 [18]
Al_2O_3 crystal <0001>	$1.8{\cdot}10^3$	$1.2{\cdot}10^{17}$		77 K	Annealing in airat 1100°C, 2 h	OA, DFWM	White *et al.* 1993 [19]
Al_2O_3 crystal	$1.5{\cdot}10^3$	$8.0{\cdot}10^{16}$	2<		Annealing in airat 500°C, 1 h	OA	Ila *et al.* 1998 [20]
Al_2O_3 crystal	25 30	$(0.2\text{-}2.0){\cdot}10^{17}$				OA, OR, TEM	Steiner *et al.* 1998 [21]
Al_2O_3 crystal	30	$3.8{\cdot}10^{17}$	3, 6, 10	RT		OA RZ-scan	Ganeev *et al.* 2005 [22] 2006 [23]
Al_2O_3 crystal	160	$(0.1\text{-}1.0){\cdot}10^{17}$				OA	Marques *et al.* 2006 [24]
ABSG, BPYR glass	270	$1.5{\cdot}10^{16}$				OA	Mazzoldi *et al.* 1993 [25]
MgO crystal (100)	180	(0.5-1.0)·1017	1	RT	Some samples annealed in vacuum at 25-1500°C	OA TEM	Abouchacra and Scrughetti 1986 [26] Fuchs et al. 1988 [27]

Table 1. (Continued)

Matrix type	Ion energy, keV	Ion dose,ion/cm2	Current density,μA/cм2	Matrix temperature,°C	Post-implantation heat treatment	Methodsof particle detection	Authors
MgO crystal (100)	$1.5 \cdot 10^3$	$1.2 \cdot 10^{17}$	2-3	27 C	Annealing in air at 550 and 1100°C	OA TEM	Qian *et al.* 1997 [28] Zimmerman *et al.* 1997 [29]
MgO crystal (100)	600	$1.0 \cdot 10^{16}$		RT	Annealing in air at 1200°C, 22 h	OA, XRD TEM-CS	van Huis *et al.* 2002 [30]
MgO crystal (100)	200	$2.0 \cdot 10^{17}$	2	RT	Some samples annealed in air, Ar, O_2 or 70%N_2 + 30%H_2, at 300-900°C, 1 h	OA, SAED TEM-CS	Xiao *et al.* 2008 [31]
$MgOP_2O_5$ glass	150	$(0.1\text{-}1.0) \cdot 10^{17}$	0.5-3	RT		OA	Matsunami and Hosono 1993 [32]
Lithia-alumina-silica glass	275-285	$1.0 \cdot 10^{16}$	1-2	300		OA	Arnold and Borders 1976 [14]
$LiNbO_3$ crystal	50 360	$(4.0\text{-}0.8) \cdot 10^{16}$	1-4	77 K 300	Annealing in air at 250-650°C, 30 min	OA	Rahmani *et al.* 1988 [17] 1989 [18]
$LiNbO_3$ crystal	20, 25 $3 \cdot 10^3$ $4.2 \cdot 10^3$	$(0.5\text{-}8.0) \cdot 10^{16}$		RT	Some samples annealed in air at 200-600°C, 1-3 h	OA OM X-ray	Deying *et al.* 1994 [33] Shang *et al.* 1996 [34] Saito and Kitahara 2000 [35] Fujita *et al.* 1994 [36]
$LiNbO_3$ crystal	160 $1.5 \cdot 10^3$	$2.0 \cdot 10^{16}$ $4.0 \cdot 10^{16}$ $1.7 \cdot 10^{17}$		RT 500	Some samples annealed in air at 500-800°C, 1 h	OA Z-scan TEM TEM-CS	Sarkisov *et al.* 1998 [27-40] 1999 [41] 2000 [42] Williams *et al.* 1998 [43, 44] 1999 [45]
$LiNbO_3$ crystal	$1.5 \cdot 10^3$	$2.0 \cdot 10^{16}$		300	Annealing in Ar gas at 100-1100°C, 30 min	OA TEM TEM-CS	Amolo *et al.* 2006 [46]
SiO2 crystal	200	(2.3-9.0)·1016	1-5	77 300	Annealing in air at 300-500°C, 30 min	OA	Rahmani and Townsend1989 [18]

Table 1. (Continued)

Matrix type	Ion energy, keV	Ion dose,ion/cm2	Current density,μA/см2	Matrix temperature,°C	Post-implantation heat treatment	Methodsof particle detection	Authors
SiO_2	65 130 270	$(1.5\text{-}5.0)\cdot10^{16}$	1 1.5	300	Some samples annealed in air or 4 % H_2 gas	OA TEM EXAFS	Mazzoldi *et al.* 1993 [47] Mazzoldi *et al.* 2005 [48] Mazzoldi *et al.* 2007 [49] Antonello *et al.* 1998 [50] Battaglin *et al.* 1998 [51] 2001 [52] Bertoncello *et al.* 1998 [53] Caccavale 1998 [54] Cattaruzza *et al.* 1999 [55] Gonella *et al.* 1999 [56]
SiO_2	150	$(0.1\text{-}6.0)\cdot10^{17}$	1.5-14	300		TEM-CS, OA	Matsunami and Hosono 1993 [57]
SiO_2	305	$(3.0\text{-}9.0)\cdot\cdot10^{16}$	2	0		OA TEM X-ray	Magruder III *et al.* 1995 [58] 1996 [59] 2009 [60] Anderson *et al.* 1996 [61] 1997 [62] 1998 [63] 2000 [64] Zuhr *et al.* 1998 [65]
SiO_2	20-58 130	$(0.4\text{-}2.0)\cdot10^{17}$	0.6	300		AFM	Pham *et al.* 1997 [66]
SiO_2 crystal	200	$(2.3\text{-}9.0)\cdot10^{16}$		300		OA TEM	Liu *et al.* 1998 [67-69]
SiO_2	$1.5\cdot10^3$	$2.0\cdot10^{16}$ $4.0\cdot10^{16}$ $1.4\cdot10^{17}$	2		Annealing in Ar gas at 500-1000°C, 1 h	OA Z-scan	Ila *et al.* 1998 [70]
SiO_2	60	$4.0\cdot10^{16}$	10	RT		OA, AFM	Stepanov *et al.* 2000 [72] 2003 [73]

Table 1. (Continued)

Matrix type	Ion energy, keV	Ion dose,ion/cm2	Current density,μA/см2	Matrix temperature,°C	Post-implantation heat treatment	Methodsof particle detection	Authors
SiO2	65	5.0·1016				X-ray EXAFS	D'Acapito and Zontone 1999 [71]
SiO_2	43 90 150 200 300	$(0.06\text{-}2.0)\cdot10^{17}$	0.8-2.5	300	Some samples annealed in air, Ar, O_2 or 70%N_2+ 30%H_2 at 300-800°C, 1 h	SAED OA, STEM TEM, EDS HRTEM TEM-CS Z-scan	Jiang *et al.* 2000 [74] Ren *et al.* 2004 [75, 76] 2005 [77-79] 2006 [80] 2007 [81] 2008 [82] 2009 [83] Liu *et al.* 2005 [84] Xiao *et al.* 2006 [85] 2007 [86, 87] Wang *et al.* 2007 [88] Wang *et al.* 2008 [89] Zhang *et al.* 2004 [90] Cai *et al.* 2008 [91] 2009 [92]
SiO_2 sol-gel film	5-100	$(5.0\text{-}6.0)\cdot10^{16}$	1.5-2.5	330 K		TEM HR-TEM XRD SAED	Armelao*et al.* 2002 [93]
SiO_2 on Si	10 30 40	$(1.0\text{-}5.0)\cdot10^{15}$ $(1.0\text{-}5.0)\cdot10^{16}$ $1.0\cdot10^{17}$	2	-	Annealing in Ar gas at 500-900°C, 1 h	OR, OR TEM-CS R TEM HR-TEM	Ishikawa *et al.* 2002 [94] 2009 [95] Tsuji *et al.* 2002 [96, 97] 2003 [98] 2004 [99] 2005 [100] Arai *et al.* 2003 [101] 2005 [102] 2006 [103] 2007 [104, 105]

Table 1. (Continued)

Matrix type	Ion energy, keV	Ion dose,ion/cm2	Current density,μA/см2	Matrix temperature,°C	Post-implantation heat treatment	Methodsof particle detection	Authors
SiO_2	$2.0 \cdot 10^3$	$(0.4\text{-}1.0) \cdot 10^{17}$	2	RT	Some samples annealed in 50%N_2 + 50%H_2 gas or in air at 230-800°C, 1 h	OA TEM HRTEM	Roiz *et al.* 2004 [106] Oliver *et al.* 2006 [107] Cheang-Wong *et al.* 2007 [108] Peña *et al.* 2007 [109] 2009 [110] Reyes-Esqueda *et al.* 2008 [111] 2009 [112] Rodrigues-Iglesias *et al.* 2008 [113] 2009 [114] Rangel-Rojo *et al.* 2009 [115]
SiO_2 on Si	40	$0.3 \cdot 10^{15}$		RT	Annealing in vacuumat 550°C, 20 min	TEM	Romanyuk *et al.* 2006 [116]
SiO_2	60	$(0.3\text{-}1.0) \cdot 10^{17}$	3	RT		OA Z-scan	Takeda *et al.* 2006 [117]
SiO_2	32-40 $1.7 \cdot 10^3$ $2.4 \cdot 10^3$	$(0.1\text{-}1.0) \cdot 10^{17}$	3-5	RT	Some samples annealed in air at 500°C, 1 h	OA TEM Z-scan	Joseph *et al.* 2007 [118, 119] Sahu *et al.* 2009 [120]
SiO_2	0.65 1.5 3 keV	$(1.2\text{-}4.7) \cdot 10^{15}$	3-5	RT		OA, OR TEM HRTEM TEM-CS	Carles *et al.* 2009 [121]
SiO_2	200	$(0.1\text{-}2.0) \cdot 10^{17}$	< 2.5	-		OA TEM TEM-CS Z-scan	Wang *et al.* 2009 [122, 123]
SiO_2+TiO	305	$6.0 \cdot 10^{16}$	7	-		OA TEM-CS	Magruder III *et al.* 2007 [124]

Table 1. (Continued)

Matrix type	Ion energy, keV	Ion dose,ion/cm2	Current density,μA/cм2	Matrix temperature,°C	Post-implantation heat treatment	Methodsof particle detection	Authors
Si3N4	20 130	4.0·1016	0.6	300		AFM	Pham et al. 1997 [66]
BPYR glass	270	1.5·1016				OA	Mazzoldi et al. 1993 [25]
Soda-lime glass	60	$2.0 \cdot 10^{16}$ $4.0 \cdot 10^{16}$	-	300	-	OR TEM-CS	Nistor *et al.* 1993 [125] Wood *et al.* 1993 [1126]
Soda-lime glass	200	$(0.5\text{-}4.0) \cdot 10^{16}$	0.5-2	RT 77 K	-	TEM TEM-CS OA	Dubiel *et al.* 1997 [127] 2000 [128] 2003 [129] 2008 [130] Seifert *et al.* 2009 [131]
Soda-lime glass	200	$(0.5\text{-}4.0) \cdot 10^{16}$	0.5-2	RT 77 K	-	TEM TEM-CS OA	Stepanov *et al.* 1998 [132] 1999 [133-135] 2000 [136-139] 2001 [140-142] 2002 [143-146] 2003 [147-149] 2004 [150, 151] 2005 [152] 2008 [153, 154] 2009 [155]
Ta_2O_5	80-130	$6.0 \cdot 10^{16}$	0.6 – 6.4	300		AFM	Pham *et al.* 1997 [66]
TiO_2 crystal	50 65	$(0.3\text{-}1.0) \cdot 10^{17}$	2	-	Annealing in Ar gas at >400°C, 1 h	OA TEM-CS	Tsuji *et al.* 2002 [156] 2003 [157]
TiO_2 Sol-gel films	30 65	$(0.1\text{-}0.5) \cdot 10^{17}$	2	RT	Annealing in Ar gas at 300-600°C, 1 h	OA	Tsuji *et al.* 2005 [158] 2006 [159]
YSZ	20 $1.5 \cdot 10^3$ $3.0 \cdot 10^3$	$(0.7\text{-}6.0) \cdot 10^{16}$	2	RT	Some samples annealed in air at 500-1000°C	OA	Saito *et al.* 2003 [160] Fujita *et al.* 2007 [161]